PHYSICAL REVIEW B VOLUME 12, NUMBER 8 15 OCTOBER 1975

Theory of the lattice energy, equilibrium structure, elastic constants, and pressure-induced phase transitions in alkali-halide crystals

Alan J. Cohen and Roy G. Gordon
Department of Chemsitry, Harvard University, Cambridge, Massachusetts 02138
(Received 28 April 1975)

The interionic forces in alkali-halide crystals are calculated theoretically, using a modified electron-gas treatment including corrections to the kinetic, exchange, and correlation energy contributions. These results are used to predict the equilibrium bond distances and lattice energies, the pressure-volume phase diagrams, and the elastic constants of the lithium, sodium, potassium, and rubidium fluorides, chlorides, bromides, and iodides. Both the $B1$ (rock salt) and $B2$ (cesium chloride) lattice types are considered, and the pressure-induced phase transition between them is predicted. First- and second-nearest-neighbor short-range interactions between the ions have been included for the $B1$ phase, while third-nearest-neighbor interactions were also needed for the $B2$ phase. The average magnitude of the deviation between the predicted and observed bond distances is 2%, lattice energy 2%, and elastic constants 10%. The pressure variation of the elastic constants for NaCl has also been predicted, up to the onset of a shear instability.

I. INTRODUCTION

The $B1$ (rocksalt)–$B2$ (cesium chloride) phase transformation in alkali-metal halides has been studied both experimentally and theoretically by a number of investigators.[1] The transformation has been found to be first order and reversible. The two principal experimental techniques which have been used to induce these structural phase changes are dynamic shock-wave compression[2] and diamond-anvil high-pressure cell[1] methods. The latter method has proved more reliable in studying the behavior of alkali-metal halides in the pressure range from 5 to 300 kbar, and in identifying definite phase transformations in KCl, KBr, KI, NaCl, RbCl, RbBr, RbI, and CsCl. A controversy had existed for some time regarding the occurrence of a transition in NaCl, since the dynamic and static methods yielded widely divergent results[3,4]; but recent studies by Fritz *et al.*[2] have resolved the problem.

The first detailed theoretical studies of the $B1$-$B2$ transformation were those of Jacobs, who employed a crude semiempirical Born-Mayer energy expansion with nearest-neighbor short-range interactions.[5] Whereas his calculated transition pressures did not agree very well with existing experimental results, certain trends such as the importance of the volume change at the transition pressure ΔV_t were recognized. More detailed Born-Mayer approaches along similar lines have been used to predict transition pressures and evaluate the cohesive energy of the $B1$ and $B2$ phases, and these are described in detail by Born and Huang[6] and by Tosi.[7] In these semiempirical treatments, the experimentally known lattice parameters and adiabatic bulk moduli (at fixed temperature) are used to determine values for parameters in the cohesive energy expansions of the two crystal phases. The transition pressures obtained by these calculations do not usually show close agreement with experiment but can serve to illustrate qualitative trends in the series of alkali halides. The spirit of these calculations has been reviewed in a recent paper by Gordon and Kim.[8]

Recently Gordon and Kim (GK) applied their electron-gas model[9] to a preliminary study of the cohesive energies of the $B1$ and $B2$ phases and the transition pressures of lithium, sodium, potassium, and rubidium fluorides, chlorides, and bromides.[8] Generally good agreement was obtained for the crystal energies of the $B1$ phase and the transition pressures with available experimental data. The present study is much more detailed in that it incorporates correction factors, which we have recently evaluated, to calculate the short-range potentials $V_s(R)$ and also evaluates the effect of second and third nearest neighbors on the crystal energies of the two phases and on the transition pressure. In addition, phase diagrams have been constructed for all the transitions and the "relative volume factors" at the transition pressure $-\Delta V_t/V_{01}$ have been evaluated, for each transition, in order to study the magnitude of the driving force and to compare with experiment.[1,10] A detailed study of the elastic constants C_{11}, C_{12}, and C_{44} of the $B1$ phase of these crystals has also been performed as has an investigation of their pressure variation in NaCl, for a knowledge of these constants and their pressure dependence is necessary to understand the nature of the forces in these crystals.

It is hoped that the present study will show how closely the electron-gas treatment describes the $B1$-$B2$ phase transformations in these crystals, will indicate which interactions are of importance, and whether or not phase changes which have yet to be observed in the laboratory will be able to be

TABLE I. Waldman-Gordon correction factors for the GK model.[a]

Ion pair	Correction factors: Kinetic	Exchange	Correlation
Li^+Li^+	1.114	0.772	0.355
Na^+Na^+	1.075	0.821	0.510
K^+K^+	1.060	0.962	0.580
Rb^+Rb^+	1.045	1.000	0.690
F^-F^-	1.075	0.821	0.510
Cl^-Cl^-	1.060	0.962	0.580
Br^-Br^-	1.045	1.000	0.690
I^-I^-	1.037	1.000	0.800
Li^+F^-	1.085	0.745	0.450
Li^+Cl^-	1.075	0.885	0.510
Li^+Br^-	1.060	0.980	0.588
Li^+I^-	1.050	0.997	0.645
Na^+F^-	1.075	0.821	0.510
Na^+Cl^-	1.068	0.916	0.550
Na^+Br^-	1.055	0.986	0.615
Na^+I^-	1.048	0.997	0.667
K^+F^-	1.068	0.916	0.550
K^+Cl^-	1.060	0.962	0.580
K^+Br^-	1.051	0.993	0.640
K^+I^-	1.045	1.000	0.690
Rb^+F^-	1.055	0.986	0.615
Rb^+Cl^-	1.051	0.993	0.640
Rb^+Br^-	1.045	1.000	0.690
Rb^+I^-	1.040	1.000	0.750

[a]Reference 12.

observed, and at what pressures these transitions should occur.

II. ELECTRON-GAS TREATMENT

The two basic assumptions of the GK model for interactions between closed-shell atoms, ions, and molecules are that the total electron density is the sum of the two separate densities, and that the non-Coulombic part of the interaction potential may be evaluated by an electron gas treatment.[9] This model has been used to obtain short-range (non-point-Coulomb) ion-ion interaction potentials $V_s(R)$ for all M^+X^-, M^+M^+, and X^-X^- interactions of importance in alkali halides MX. These short-range potentials contain contributions from electronic kinetic energy, exchange energy, and correlation energy (as well as other effects). Recently there have been many modifications of the GK procedure which attempt to correct the electron-gas exchange and correlation-energy expressions to show better agreement with gas-phase experimental data.[11] These treatments attempt to correct deficiencies in the model itself rather than to merely introduce semiempirical parameters to be found by comparing with experiment. Gordon, Cohen, and Waldman have been interested in this problem of correction factors and have sought, in the spirit of Slater's $X\alpha$ method, factors α_i of the form

$$E_{\text{kin}}^{\text{corr}} = \alpha_{\text{kin}} E_{\text{GK}}, \tag{1}$$

similarly for the exchange and correlation energies. The correction factors used in calculating the gas-phase ion-ion potentials that have been employed in the present study are listed in Table I. These factors have been calculated by Gordon and Waldman following a new procedure to be discussed in detail elsewhere.[12]

Using these corrected short-range potentials, three more assumptions have been made: (a) The crystals are composed of the free ions. (b) The interactions of ions are pairwise additive and many-body effects may be neglected. (c) The short-range interactions may for the $B1$ phase be restricted to first and second nearest neighbors, while in the $B2$ phase first-, second-, and third-nearest-neighbor interactions must be considered. This is because in the $B2$ phase first and second nearest neighbors are at approximately equal separations from a given ion and hence may be collectively regarded as "pseudo-first" nearest neighbors. In addition, there are many third nearest neighbors at a slightly larger separation which should be considered.

With these assumptions the energies of the $B1$ and $B2$ phases, per M^+X^- pair, relative to stationary separated free ions (in a.u.), are

$$E_{B1}(R) = -\frac{1.747558}{R} + 6V_s(R)_{M^+X^-} + 6V_s(\sqrt{2}R)_{M^+M^+} + 6V_s(\sqrt{2}R)_{X^-X^-}, \tag{2}$$

and

$$E_{B2}(R) = -1.76268/R + 8V_s(R)_{M^+X^-} + 3V_s(2R/\sqrt{3})_{M^+M^+} + 3V_s(2R/\sqrt{3})_{X^-X^-} + 6V_s(2\sqrt{\tfrac{2}{3}}R)_{M^+M^+} + 6V_s(2\sqrt{\tfrac{2}{3}}R)_{X^-X^-}, \tag{3}$$

where R is the nearest-neighbor separation and the first term in each expansion is the Madelung energy contribution. The Madelung constants of Johnson[8] have been employed in the present study. The expansions do not contain the realtively small zero-point energy contributions, and since all calculations have been performed at 0 °K, thermal energy contributions were not considered.

Equations (2) and (3) have been used to determine equilibrium internuclear separations and cohesive energies of the two phases at 0 °K. These results are summarized in Tables II and III where a comparison with the uncorrected GK model,[8] and experimental results[7,13] has been made. The results for both a corrected-first-nearest-neighbor GK treatment and the full expansions given in Eqs. (2) and (3) are shown. These results are discussed in detail in Sec. V.

TABLE II. Equilibrium properties of some alkali-halide crystals in the $B1$ phase. R and D_e are the nearest-neighbor distance and cohesive energy of the crystal.

	R (Å)				D_e (kcal/mole)				
	Calculated			Experimental	Calculated			Experimental	
	GK[c]	Present $B1$-1[a]	Present $B1$-2[b]	0 °K[d]	GK[c]	Present $B1$-1[a]	Present $B1$-2[b]	0 °K[e]	(298 °K)[d]
LiF	1.93	2.01	2.13	2.014	260.2	249.4	240.5	246.8	(242.3)
LiCl	2.47	2.52	2.60	2.570	206.1	201.0	202.0	201.8	(198.9)
LiBr	2.66	2.68	2.73	2.751	192.3	189.5	194.9		(189.8)
LiI		2.95	2.90	3.000		172.6	186.4		(177.7)
NaF	2.31	2.42	2.44	2.317	222.3	212.5	211.9	217.9	(214.4)
NaCl	2.86	2.93	2.93	2.820	182.7	176.7	179.9	185.3	(182.6)
NaBr	3.04	3.08	3.05	2.989	172.6	168.4	173.8	174.3	(173.6)
NaI		3.34	3.25	3.237		155.3	164.9	162.3	(163.2)
KF	2.60	2.71	2.71	2.674	204.1	194.0	194.4	194.5	(189.8)
KCl	3.05	3.16	3.14	3.147	175.3	167.4	170.1	169.5	(165.8)
KBr	3.20	3.29	3.25	3.298	167.2	161.0	165.4	159.3	(158.5)
KI		3.52	3.44	3.533		150.6	158.0	151.1	(149.9)
RbF	2.77	2.84	2.83	2.815	194.0	187.2	188.1		(181.4)
RbCl	3.19	3.28	3.26	3.291	169.4	162.6	165.0		(159.3)
RbBr	3.32	3.43	3.39	3.445	161.9	156.1	159.8		(152.6)
RbI		3.66	3.58	3.671		146.6	152.7		(144.9)

[a]Calculated using correction factors given in Table I but only using first nearest neighbors.
[b]Calculated using correction factors given in Table I and Eq. (2).
[c]Reference 8. Only first nearest neighbors and no correction factors were considered.
[d]Data compiled by Tosi, Ref. 7, p. 44.
[e]Extrapolated to 0 °K by L. Brewer, quoted by Kittel, Ref. 13, p. 121.

III. THERMODYNAMICS OF THE $B1$-$B2$ TRANSITIONS

The $B1$-$B2$ phase transformations were studied at 0 °K because of the simplicity of the calculations and because these phase changes are experimentally known to exhibit very little temperature dependence.[8,14] At 0 °K the (Gibbs) free energies of the two phases (per M^+X^- pair) are

$$G_{B1}(R) = E_{B1}(R) + 2R^3P \tag{4}$$

and

$$G_{B2}(R') = E_{B2}(R') + \frac{8}{3\sqrt{3}}R'^3P, \tag{5}$$

TABLE III. Parameters for alkali-halide crystals in the $B2$ phase. The last three columns show energy differences between the $B1$ and $B2$ phases at 0 °K.[a] [Calculated using correction factors and Eqs. (2) and (3)].

	R[b] (a.u.)			D_e[b] (a.u.)			$D_e(B1)$		
	GK[c]	Present $B2$-1[d]	Present $B2$-2[e]	GK[c]	Present $B2$-1[d]	Present $B2$-2[e]	(kcal/mole)	$D_e(B2)$	$\Delta D_e(B1$-$B2)$
LiF	3.83	3.98	4.36[f]	0.4007	0.3837	0.3568[f]	240.5	223.9[g]	16.6
LiCl	4.87	4.99	5.29	0.3187	0.3107	0.3037	202.0	190.6	11.4
LiBr	5.24	5.30	5.56	0.2978	0.2932	0.2939	194.9	184.4	10.5
LiI		5.82	5.84		0.2672	0.2868	186.4	180.0	6.4
NaF	4.56	4.75	4.89	0.3449	0.3295	0.3237	211.9	203.1	8.8
NaCl	5.61	5.75	5.83	0.2847	0.2749	0.2772	179.9	173.9	6.0
NaBr	5.92	6.05	6.08	0.2690	0.2621	0.2690	173.8	168.8	5.0
NaI		6.55	6.43		0.2418	0.2589	164.9	162.5	2.4
KF	5.07	5.29	5.35	0.3197	0.3030	0.3021	194.4	189.5	4.9
KCl	5.95	6.16	6.18	0.2753	0.2620	0.2656	170.1	166.7	3.4
KBr	6.22	6.42	6.40	0.2626	0.2522	0.2594	165.4	162.8	2.6
KI		6.87	6.74		0.2360	0.2510	158.0	157.5	0.5
RbF	5.37	5.54	5.60	0.3050	0.2935	0.2930	188.1	183.8	4.3
RbCl	6.18	6.40	6.39	0.2668	0.2554	0.2593	165.0	162.7	2.3
RbBr	6.48	6.67	6.63	0.2549	0.2454	0.2523	159.8	158.3	1.5
RbI		7.12	6.97		0.2305	0.2438	152.7	153.0	−0.3

[a]Calculated using correction factors and Eqs. (2) and (3).
[b]R and D_e are the nearest-neighbor distance and cohesive energy of the crystal.
[c]Ref. 8. Only first nearest neighbors and no correction factors were considered.
[d]Calculated using correction factors given in Table I but only using first nearest neighbors.
[e]Calculated using correction factors given in Table I and Eq. (3).
[f]Calculated using correction factors given in Table I but only the first four terms in Eq. (3).
[g]Only first- and second-nearest-neighbor short-range interactions included.

TABLE IV. Transition pressures of some alkali-halide crystals ($B1 \rightarrow B2$) (in kbar).

	Semiempirical	GK[c]	Present work[a] (1st nn)	Present work[b]	Experimental	Values[e,f,i]
LiF	310[d]	550	480	2900	>100[d,e]	
LiCl	140[d]	160	144	980	>100[d]	
LiBr	105[d]	110	105	924	>100[d]	
LiI	68[d]		67	184	>100[d]	
NaF	200[d]	142	129	326	>200[e]	
NaCl	74[d]	49	49	107	300[g]	
NaBr	53[d]	35	39	79	>100[d]	
NaI	39[d]		27	23	>100[d]	
KF	88[d]	51	51	85	>100[d]	20[e]
KCl	36[d] 21.6[j]	21	24	34	20[d]	19.7[e] 21[h]
KBr	29[d] 19.0[j]	17.0	19.0	23	19[d]	18.1[e] 18.5[e]
KI	21[d] 18.8[j]		14.0	3.6	17.8[i]	
RbF	68[d]	30	32	65	>100[d]	11.8[e]
RbCl	31[d] 6.3[j]	14.0	15.9	17.1	5.5[d]	4.9[e]
RbBr	25[d] 5.2[j]	12.4	12.4	9.7	5.0[d]	4.5[e]
RbI	15[d] 5.1[j]		9.1		3.4[i]	4.0[i]

[a]A corrected first-nearest-neighbor treatment.

[b]Using correction factors and full Eq. (2) and (3) except for LiF where only first four terms in Eq. (3) were used.

[c]Reference 8.

[d]Reference 6, p. 162.

[e]"> 100" means no transitions were found below 100 kbar.

[f]See Ref. 8 for a more complete summary.

[g]Reference 3.

[h]Reference 1.

[i]See Ref. 32 for a variety of values.

[j]See Ref. 7. These are *not* predictions, for experimental parameters at the experimental transition pressures were used to obtain energy equations for the two phases.

where R and R' are the nearest-neighbor M^+X^- separations in these phases. By minimizing the free energies with respect to internuclear separations at fixed applied pressure, free-energy changes

$$\Delta G = G_{B2} - G_{B1} \tag{6}$$

have been calculated. Below the transition pressure, for the crystals we have studied, the $B1$ phase is more stable; hence ΔG is positive, whereas as the transition pressure is approached, ΔG approaches zero and the two phases "stand in equilibrium." Above the transition pressure, ΔG becomes negative as the $B2$ phase becomes the more stable one.

Using a minimization interpolation procedure we were able to locate transition pressures usually to within 1% uncertainty. These transition pressures are summarized in Table IV where a comparison with the uncorrected GK model,[8] semiempirical calculations,[6] and various experiments has been made.[8,10] Complete phase diagrams for these first-order phase changes obtained by a first-nearest-neighbor corrected GK treatment and from the complete expansions (2) and (3) appear as Figs. 1–16.

Experimentally, one usually studies the relative volumes changes $-\Delta V/V_{01}$ associated with the compressions. These are defined as[1] the negative of the difference between the volume of the more stable phase at a given pressure and the volume of the $B1$ phase at zero applied pressure V_{01} divided

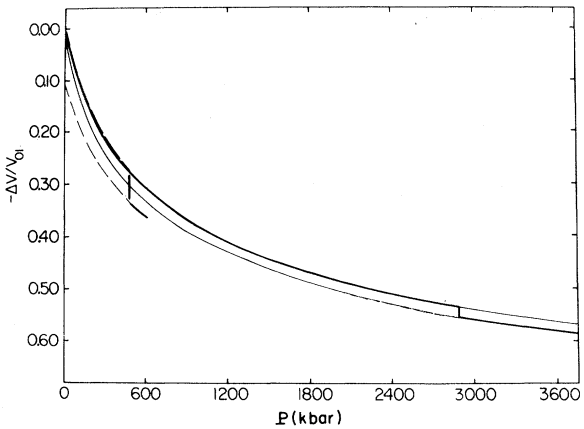

FIG. 1. Phase diagram for LiF: – – – First-nearest-neighbor-corrected GK model; —— Full expansion treatment using Eqs. (2) and (3). Dark lines indicate regions of stability, and light lines indicate regions of metastability.

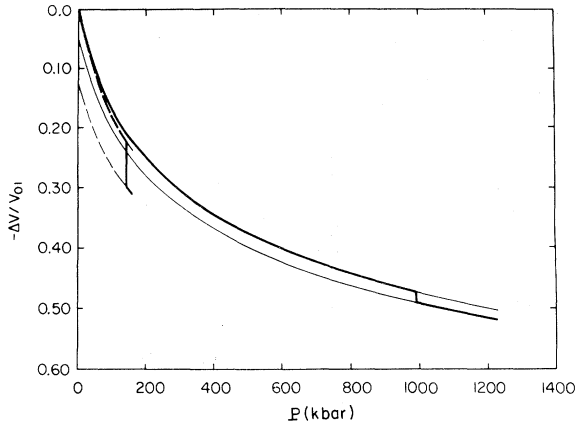

FIG. 2. Phase diagram for LiCl.

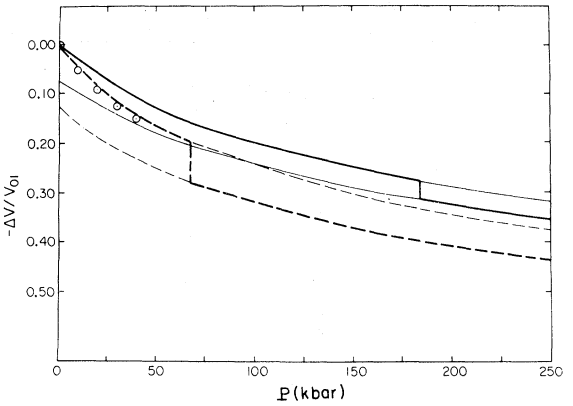

FIG. 4. Phase diagram for LiI: Experimental data from Vaidya and Kennedy, Ref. 32. (shown as circles).

by V_{01}. It is useful to define $-\Delta V_t/V_{01}$ by[1]

$$-\Delta V_t/V_{01} = (V_{t1} - V_{t2})/V_{01}, \tag{7}$$

where V_{ti} is the volume of phase Bi at the transition pressure, and $-\Delta V_t/V_{01}$ is, of course, the magnitude of the discontinuity in $-\Delta V/V_{01}$ in the first-order phase diagrams. The factors $-\Delta V_t/V_{01}$ have been computed directly or obtained from the phase diagrams and appear with available experimental results in Table V. A full discussion of the significance of these results appears in Sec. V.

IV. ELASTIC CONSTANTS OF ALKALI HALIDES

Valuable information about the nature of forces in the $B1$ phase of alkali-halide crystals may be obtained from a study of the three elastic constants C_{11}, C_{12}, and C_{44}. Since these constants are functions of the first and second derivatives of our short-range potentials $V_s(R)$, a calculation of them can provide a further check on the accuracy of the electron-gas description of the actual short-range forces in these crystals. The calculations, performed at 0 °K and zero applied pressure, are also important because measurements of these constants, usually by ultrasonic methods,[13,15] are often difficult to perform accurately and only a few of the measurements have been extrapolated to the 0 °K regime.

To calculate these constants, it is useful to partition them into contributions from Coulombic and short-range forces. Thus

$$C_{11} = C_{11}^{\text{Coul}} + C_{11}^{\text{sr}}, \tag{8}$$

similarly for C_{12} and C_{44}. The Coulombic contributions involve summations over all interactions in the crystal, whereas the short-range contributions may be restricted to first and second nearest neighbors. Blackman,[16] following a treatment similar to that developed by Fuchs[17] for metals, derived general expresssions for the elastic constants in cubic ionic crystals. These appear as

$$C_{11} = \frac{1}{v}\sum_l [Q(X^l)^4 + P(X^l)^2], \tag{9}$$

$$C_{12} = \frac{1}{v}\sum_l [Q(X^l)^2(y^l)^2 - P(X^l)^2], \tag{10}$$

$$C_{44}^* = \frac{1}{v}\sum_l [Q(X^l)^2(y^l)^2 + P(X^l)^2], \tag{11}$$

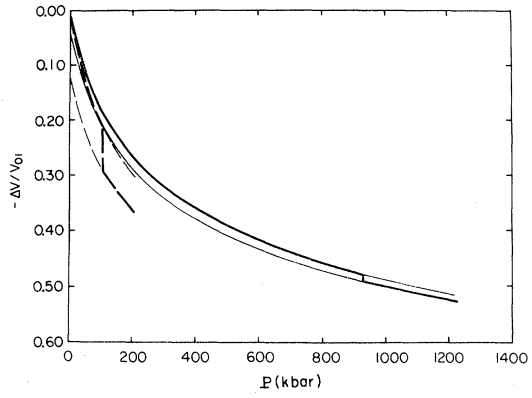

FIG. 3. Phase diagram for LiBr.

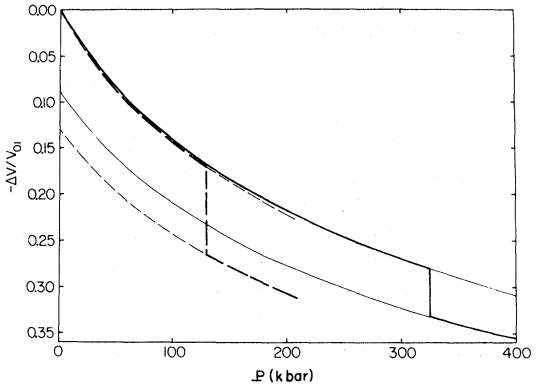

FIG. 5. Phase diagram for NaF.

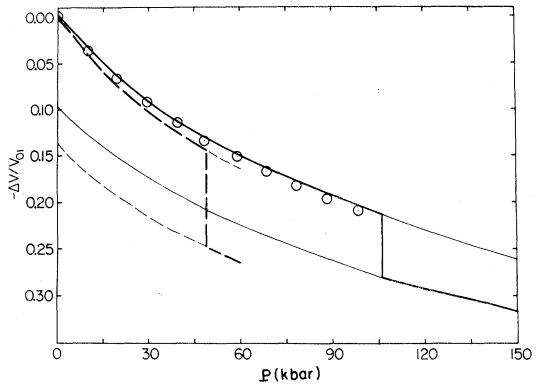

FIG. 6. Phase diagram for NaCl: Experimental data (shown as circles) from Bridgman, Ref. 10.

$$C_{44} = C_{44}^{*} - C^2/D, \tag{12}$$

with

$$C = \frac{1}{v}\sum_l X^l y^l z^l Q, \tag{13}$$

$$D = \frac{1}{v}\sum_l [P + Q(X^l)^2], \tag{14}$$

where v, the volume per ion pair, is $2R^3$ for the $B1$ phase, $(X/R,\ y/R,\ z/R)$ are the coordinates of the lattice sites in the crystallographic cell, and the summations extend over all interactions of importance as we have described above. In these equations, P and Q are defined as

$$P = \left(\frac{1}{r}\frac{d}{dr}E_{B1}^l(r)\right)_{R'}, \tag{15}$$

$$Q = \left[\frac{1}{r}\frac{d}{dr}\left(\frac{1}{r}\frac{dE_{B1}^l(r)}{dr}\right)\right]_{R'}, \tag{16}$$

where $E_{B1}^l(r)$ is the two-body potential[18,19] in (2) appropriate at R'.

The Coulombic contributions to these elastic constants may be obtained from the first term of Eq. (2). The actual calculation requires the use of rapidly convergent summation techniques, as have been described in detail by Tosi[7] and Huntington.[15] The results of calculations performed by Cowley[18] using these methods are summarized below (in a.u.).

$$C_{11}^{\mathrm{Coul}} = -2.55604/2R^4, \tag{17}$$

$$C_{12}^{\mathrm{Coul}} = 0.11298/2R^4, \tag{18}$$

$$C_{44}^{\mathrm{Coul}} = C_{44}^{*\mathrm{Coul}} = 1.27802/2R^4, \tag{19}$$

where R is the nearest-neighbor equilibrium separation, and the optical constant D is given by[18]

$$D^{\mathrm{Coul}} = -4.189/2R^6. \tag{20}$$

The first detailed treatment of the contribution of short-range forces in the $B1$ phase to elastic constants was performed by Anderson and Liebermann[19] who derived equations for an arbitrary first-nearest-neighbor potential $V_s(R)_{M^+X^-}$, (henceforth referred to as V_{+-}), and later restricted this to a semiempirical inverse-nth-power potential. Re-

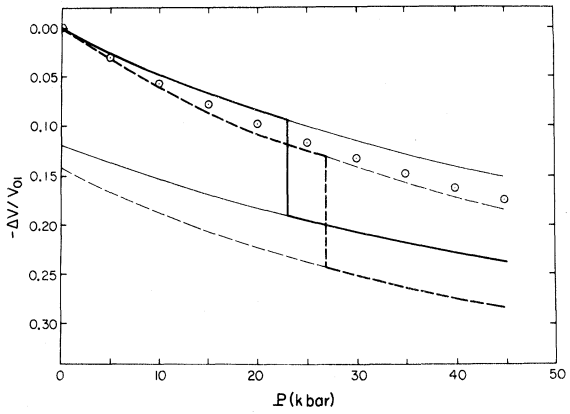

FIG. 8. Phase diagram for NaI: Experimental data from Ref. 10.

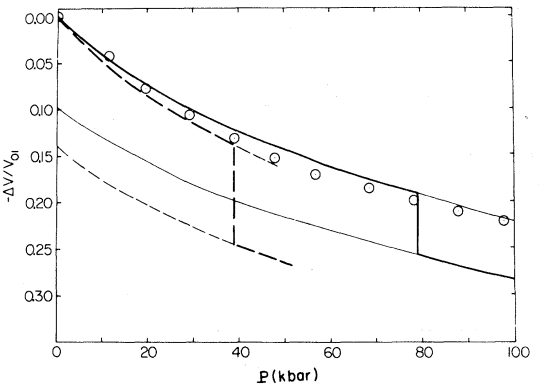

FIG. 7. Phase diagram for NaBr: Experimental data from Ref. 10.

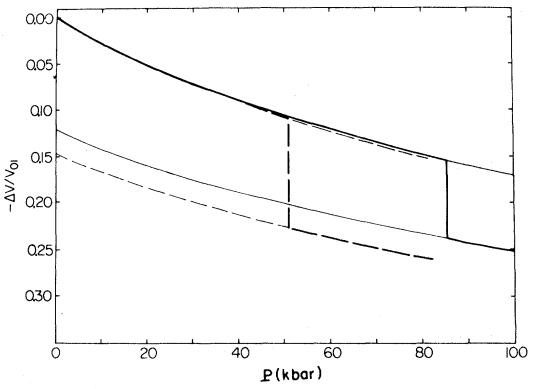

FIG. 9. Phase diagram for KF.

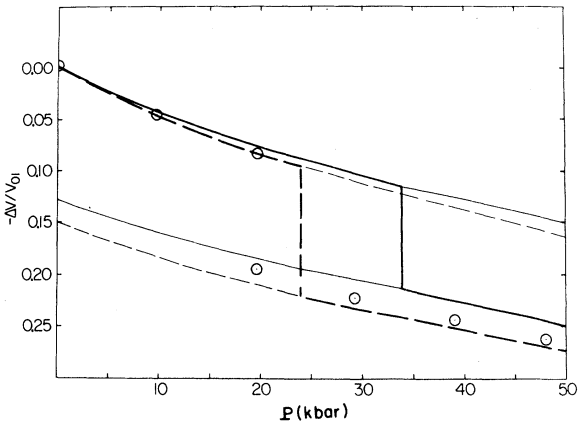

FIG. 10. Phase diagram for KCl: Experimental data from Ref. 10.

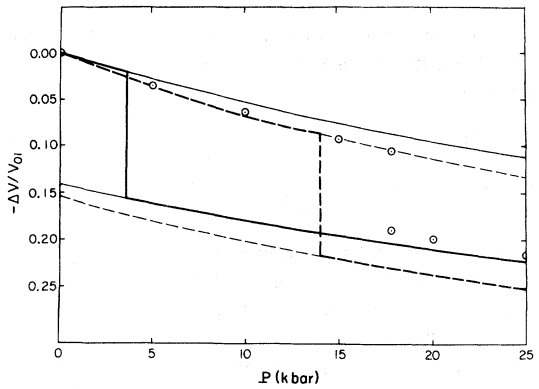

FIG. 12. Phase diagram for KI: Experimental data from Ref. 10.

cently, Spetzler *et al.*[20] repeated the calculations for NaCl using an exponential $Ae^{-r/\rho}$ potential, and they also attempted to include second-nearest-neighbor $Cl^- - Cl^-$ interactions using an Ar – Ar (solid) isoelectronic van der Waals potential; however, general equations for the contributions of general $V_s(\sqrt{2}R)_{M^+M^+}$ and $V_s(\sqrt{2}R)_{X^-X^-}$ potentials (henceforth referred to as V_{++} and V_{--}) to the elastic constants were not derived. The effect of second nearest neighbors may be included using Eqs. (9)–(16) and (2); in fact, following a different approach, Woods *et al.*[21] derived an analogous set of equations to include those desired interactions. The resulting equations for the electron gas short-range contributions to the elastic constants and optical constant D of the $B1$ phase appear below.

$$C_{11}^{sr}=\frac{1}{R}\left(\frac{d^2V_{+-}}{dr^2}\right)_R+\frac{1}{R}\left(\frac{d^2(V_{++}+V_{--})}{dr^2}\right)_{\sqrt{2}R}+\frac{1}{\sqrt{2}R^2}\left(\frac{d}{dr}(V_{++}+V_{--})\right)_{\sqrt{2}R}, \tag{21}$$

$$C_{12}^{sr}=\frac{-1}{R^2}\left(\frac{dV_{+-}}{dr}\right)_R+\frac{1}{2R}\left(\frac{d^2(V_{++}+V_{--})}{dr^2}\right)_{\sqrt{2}R}-\frac{5}{2\sqrt{2}R^2}\left(\frac{d}{dr}(V_{++}+V_{--})\right)_{\sqrt{2}R}, \tag{22}$$

$$C_{44}^{sr}=\frac{1}{R^2}\left(\frac{dV_{+-}}{dr}\right)_R+\frac{1}{2R}\left(\frac{d^2(V_{++}+V_{--})}{dr^2}\right)_{\sqrt{2}R}+\frac{3}{2\sqrt{2}R^2}\left(\frac{d}{dr}(V_{++}+V_{--})\right)_{\sqrt{2}R}, \tag{23}$$

$$D^{sr}=\frac{2}{R^4}\left(\frac{dV_{+-}}{dr}\right)_R+\frac{1}{R^3}\left(\frac{d^2V_{+-}}{dr^2}\right)_R+\frac{1}{R^3}\left(\frac{d^2}{dr^2}(V_{++}+V_{--})\right)_{\sqrt{2}R}+\frac{2}{\sqrt{2}R^4}\left(\frac{d}{dr}(V_{++}+V_{--})\right)_{\sqrt{2}R}. \tag{24}$$

In the above equations, r is the appropriate distance variable for each pair. Results of calculations using Cowley's ionic terms and Eqs. (21)–(23) in the electron-gas approximation [using both first-nearest-neighbor-corrected GK potentials and the full expansions (21)–(23)] appear in Table

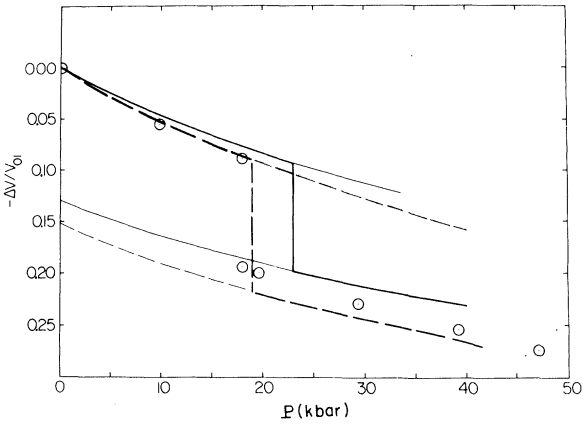

FIG. 11. Phase diagram for KBr: Experimental data from Ref. 10.

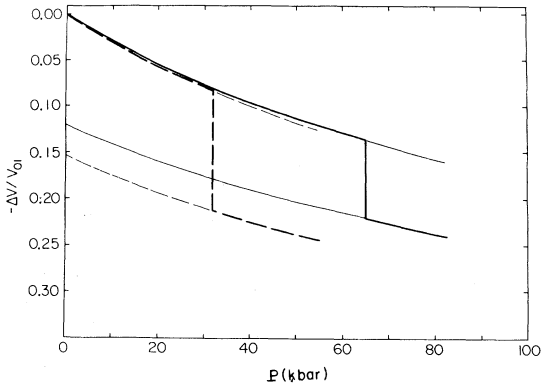

FIG. 13. Phase diagram for RbF.

VI and are discussed in Sec. V. In this table values for the shear constant C' and the bulk modulus B, defined by

$$C' = \tfrac{1}{2}(C_{11} - C_{12}), \tag{25}$$

$$B = \tfrac{1}{3}(C_{11} + 2C_{12}) = \frac{1}{18R}\left(\frac{d^2E}{dR^2}\right)_{\text{equil}}, \tag{26}$$

are also listed and the results of preliminary calculations of B by Gordon and Kim[8] using an uncorrected GK model and experimental results[22] are also summarized.

In addition, we have used the results of our phase-transition study for NaCl as given in Fig. 6 and Eqs. (17)–(19) and (21)–(23) to evaluate C_{11}, C_{12}, and C_{44} as a function of pressure up to the onset of a shear instability ($C_{44} = 0$). These results are summarized in Figures 17–19 and are discussed in Sec. V.

V. DISCUSSION OF RESULTS

A. Cohesive-energy calculations

The results of a corrected-first-nearest-neighbor GK and "complete" expansion treatment based on Eqs. (2) and (3), of the equilibrium properties of the $B1$ and $B2$ phases of the sixteen alkali halides, appear in Tables II and III and show excellent agreement with experiment. Whereas the uncorrected GK model[8] generally overestimates the cohesive energy of the $B1$ phase the present calculations are generally slightly less than the experimental energies at 0 °K.

Errors in the calculations, besides those inherent in the electron-gas approximation, may be attributed to a neglect of many body interactions in the crystals and to an incomplete description of dispersion forces. The correlation energy contribution to $V_s(R)$ is only roughly equal to the long-range van der Waals dispersion force,[11] so that

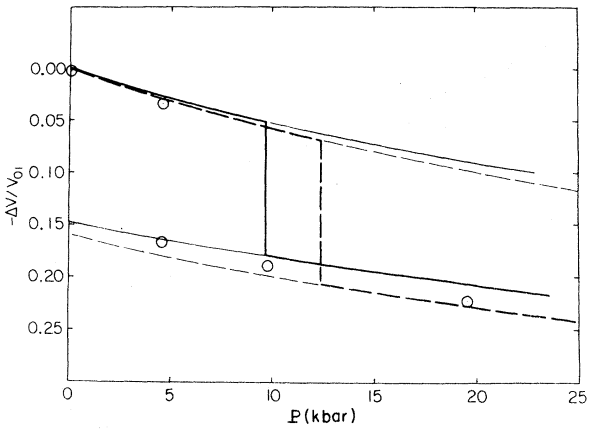

FIG. 15. Phase diagram for RbBr: Experimental data from Ref. 10.

dispersion effects have not been rigorously accounted for in our calculations. Nevertheless, the sum of zero-point energy and dispersion terms in alkali halides has been shown, by various semiempirical treatments, to be a very small stabilizing contribution to the crystal energy of the $B1$ phase and of slightly greater importance in the $B2$ phase.[6] Since this stabilizing contribution accounts for a few percent of the crystal-lattice energy, we should expect the energy expansions to underestimate the experimental 0 °K lattice energy by a few percent. Table II indicates this to generally be the case. Incorporation of dispersion and zero-point contributions in our expansions should in most cases give even better agreement with experiment; however, to incorporate dispersion forces rigorously into the present calculations would require a knowledge of accurate ion-ion C_6 coefficients, which does not presently exist.

The effect of second and third nearest neighbors

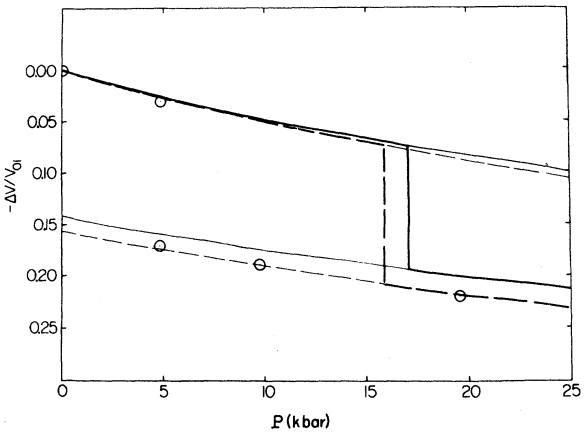

FIG. 14. Phase diagram for RbCl: Experimental data from Ref. 10.

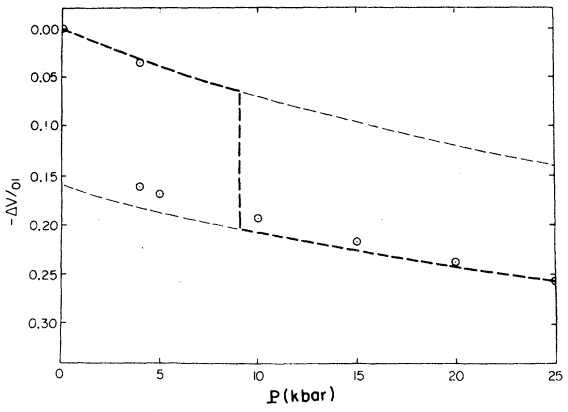

FIG. 16. Phase diagram for RbI: – – – First nearest neighbor corrected GK model: Experimental data (shown as circles) from Bridgman, Ref. 10.

TABLE V. Comparison of the electron-gas volume data with experiment.

	Present study (at theoretical transition pressures)			Experimental results (at experimental transition pressures)		
	$-\Delta V_{B1}/V_{01}$	$-\Delta V_{B2}/V_{01}$	$(-\Delta V_t/V_{01})$	$-\Delta V_{B1}/V_{01}$	$-\Delta V_{B2}/V_{01}$	$(-\Delta V_t/V_{01})$
LiF	0.275[a]	0.335	0.060		[c]	
	0.533[b]	0.553	0.020			
LiCl	0.223[a]	0.298	0.076		[c]	
	0.475[b]	0.492	0.017			
LiBr	0.212[a]	0.290	0.078		[c]	
	0.478[b]	0.492	0.014			
LiI	0.196[a]	0.281	0.085		[c]	
	0.276[b]	0.315	0.039			
NaF	0.172[a]	0.266	0.094			
	0.280[b]	0.332	0.053		[c]	
NaCl	0.145[a]	0.249	0.104	0.357	0.394	0.037[d]
	0.214[b]	0.281	0.067			
NaBr	0.140[a]	0.246	0.106		[c]	
	0.189[b]	0.257	0.068			
NaI	0.132[a]	0.242	0.110		[c]	
	0.093[b]	0.190	0.097			
KF	0.110[a]	0.228	0.118		[c]	
	0.153[b]	0.239	0.086			
KCl	0.096[a]	0.220	0.124	0.085	0.197	0.112[e]
	0.116[b]	0.216	0.100	0.098	0.211	0.113[f]
KBr	0.090[a]	0.217	0.127	0.088	0.193	0.105[e]
	0.093[b]	0.198	0.105			
KI	0.086[a]	0.215	0.129	0.105	0.190	0.085[e]
	0.022[b]	0.157	0.135			
RbF	0.084[a]	0.214	0.130		[c]	
	0.135[b]	0.220	0.085			
RbCl	0.075[a]	0.209	0.134	0.030	0.170	0.140[e]
	0.073[b]	0.193	0.120			
RbBr	0.070[a]	0.208	0.138	0.033	0.166	0.133[e]
	0.052[b]	0.178	0.126			
RbI	0.065[a]	0.205	0.140	0.030	0.158	0.128[g]
				0.035	0.161	0.126[e]

[a]Corrected GK first-nearest-neighbor calculation.
[b]From Eqs. (2) and (3).
[c]No available data or transition not found.
[d]Reference 3.
[e]Reference 10.
[f]Reference 1.
[g]Reference 32.

on the cohesive energies of the crystal phases can be seen from Tables II and III. Contributions due to short-range interactions from neighbors at even larger separations are insignificant. At rather short separations, such as in LiF, many-body interactions should be considered. Semiempirical studies have shown nonadditive three-body ion-ion interactions to be of importance in this crystal,[23] and covalent effects are also likely to be important. Thus for LiF, only a simplified treatment[7] using the first four terms in Eq. (3) was performed to study the properties of the $B2$ phase. For LiF, inclusion of second nearest neighbors in the $B1$ phase leads to a less stable structure. This is primarily due to anion-anion interactions at short distances. In most of the other crystals, the second-nearest-neighbor separations are sufficiently large that the effect of these neighbors is to stabilize the structure, this being largely due to stabilizing electron exchange and correlation effects in the crystal.

The most important second- (and third-) nearest-neighbor interactions in these crystals are of the anion-anion type. This was determined by comparing the results of calculations based on Eqs. (2) and (3) with calculations which omitted cation-cation short-range interactions from these expansions.[24] As expected, only in the case of the rubidium halides, particularly rubidium fluoride, does inclusion of cation-cation interactions greatly affect the cohesive energy of the crystal. This is, of course, expected, due to the large ionic radius of the Rb^+ ion relative to that of F^-. In fact, the calculations show that in these crystals F^-F^- interactions are generally of a charge-cloud-repulsion type, in contrast to Cl^-Cl^-, Br^-Br^-, and I^-I^- interactions which, being at larger separations, often tend by electron exchange and correlation interac-

TABLE VI. Elastic constants of alkali halides ($B1$ phase).

	C_{11} (10^{11} dyne/cm^2)			C_{12}			C_{44}			B				C'		
	Calculated			Calculated			Calculated				Calculated			Calculated		
	$B1$-1[a]	$B1$-2[b]	Expt.[c]	$B1$-1[a]	$B1$-2[b]	Expt.[c]	$B1$-1[a]	$B1$-2[b]	Expt.[c]	GK[d]	$B1$-1[a]	$B1$-2[b]	Expt.[c]	$B1$-1[a]	$B1$-2[b]	Expt.[c]
LiF	12.91	8.17	13.90*[h]	4.95	6.50	6.05*[h]	4.95	6.50	6.84*[h]	9.3	7.61	7.06	8.67*[h]	3.98	0.83	3.92*[h]
LiCl	5.99	5.45	6.07[g]	1.98	2.77	2.27[g]	1.98	2.77	2.69[g]	3.6	3.32	3.66	3.54[g]	2.01	1.34	1.90[g]
LiBr	4.86	5.21	e	1.54	2.27	e	1.54	2.27	e	2.70	2.65	3.25	e	1.66	1.47	e
LiI	3.52	5.36	e	1.05	1.48	e	1.05	1.48	e		1.87	2.11	e	1.24	1.94	e
NaF	8.66	8.08	10.85[g]	2.36	2.78	2.29[g]	2.36	2.78	2.90[g]	5.3	4.46	4.55	5.14[g]	3.15	2.65	4.28[g]
NaCl	4.38	4.86	6.00*[f]	1.09	1.27	1.27*[f]	1.09	1.27	1.40*[f]	2.42	2.18	2.46	2.85*[f]	1.65	1.79	2.37*[f]
NaBr	3.71	4.56	4.90*[g]	0.89	1.03	0.98*[g]	0.89	1.03	1.09*[g]	2.19	2.18	2.21	2.29*[g]	1.41	1.77	1.96*[g]
NaI	2.78	4.21	3.95*[l]	0.64	0.66	0.59*[l]	0.64	0.66	0.80*[l]		1.35	1.85	1.71*[l]	1.07	1.78	1.83*[l]
KF	6.95	7.08	7.57[g]	1.49	1.61	1.35[g]	1.49	1.61	1.34[g]	3.8	3.31	3.43	3.42[g]	2.73	2.74	3.11[g]
KCl	3.97	4.44	5.02*[i]	0.81	0.85	0.52*[i]	0.81	0.85	0.68*[i]	2.25	1.86	2.05	2.02*[i]	1.58	1.80	2.25*[i]
KBr	3.43	4.16	4.30*[j]	0.68	0.70	0.55*[j]	0.68	0.70	0.57*[j]	1.7	1.60	1.86	1.80*[j]	1.38	1.73	1.88*[j]
KI	2.70	3.79	3.44*[i]	0.52	0.47	0.22*[i]	0.52	0.47	0.37*[i]		1.28	1.58	1.29*[i]	1.09	1.66	1.61*[i]
RbF	6.41	6.70	e	1.24	1.30	e	1.24	1.30	e	3.3	2.96	3.10	e	2.59	2.70	e
RbCl	3.74	4.18	4.50*[k]	0.69	0.69	0.52*[k]	0.69	0.69	0.50*[k]	1.9	1.71	1.85	1.85*[k]	1.53	1.74	1.99*[k]
RbBr	3.32	3.74	3.97*[k]	0.58	0.56	0.40*[k]	0.58	0.56	0.41*[k]	1.9	1.49	1.62	1.59*[k]	1.37	1.59	1.58*[k]
RbI	2.56	3.44	3.24*[k]	0.45	0.38	0.29*[k]	0.45	0.38	0.30*[k]		1.15	1.40	1.27*[k]	1.06	1.53	1.48*[k]

[a]Calculated using correction factors given in Table I but only using first nearest neighbors.

[b]Calculated using correction factors given in Table I and the full Eqs. (21)–(23).

[c]Either an experimental measurement at 4.2 °K, or an extrapolation of literature values to 0 °K from $T > \Theta_D$ (denoted by an asterisk).

[d]Reference 8. Rather large uncertainties existed due to the numerical procedure employed.

[e]Only room-temperature values exist and no extrapolation is possible, see Ref. 22.

[f]Reference 20.

[g]Reference 26.

[h]Reference 30.

[i]Reference 28.

[j]Reference 29.

[k]Reference 33.

[l]Reference 34.

tions to stabilize the crystal.

Our cohesive-energy calculations show that the complete expansion treatment accurately describes the forces in the $B1$ and $B2$ phases of the alkali halides except for KI and RbI; indeed a first-nearest-neighbor treatment appears far superior for those two cases. The rather large I^-I^- separations in these crystals, at which the short-range electron-gas description is poorest, contribute to the disagreement with experiment and to the apparently low electron-gas energy differences between the two phases. For LiI and NaI where the I^-I^- interactions are at shorter separations the complete expansion treatment shows much better agreement with experiment.

The cohesive-energy differences for the alkali halides crystallized in the $B1$ and $B2$ lattices are summarized in Table III. It is thus seen that as one proceeds down the table toward CsCl (which is known to crystallize in the $B2$ phase but which has not been studied by the GK model because accurate analytical Cs^+ wave functions do not exist), the $B2$ phase begins to become almost as stable as the $B1$ phase. The rather low-energy differences between phases for KBr, KCl, RbBr, and RbCl would indicate that it might be possible, under applied pressures, for example, for these halides to crystallize in the $B2$ phase. Indeed high-pressure studies[1] have shown this to be the case, as will be discussed more fully below. In contrast, it is not surprising that LiF has not been experimentally observed to crystallize in the $B2$ lattice under any experimental conditions.

B. Polymorphic-transition calculations

The polymorphic transitions of KCl, KBr, KI, RbCl, RbBr, and RbI have been observed experimentally, generally using diamond-anvil high-pressure cells.[1] These are known to occur in the pressure range from 4 to 25 kbar and to exhibit kinetic effects, displaying a region of indifference about the transiton pressure. In addition, they are all known to have relatively large relative volume factors at the transition pressure. The low-transition pressures for these crystals can in part be rationalized by the low-energy differences between the two phases in these systems, as we have described above.

The results of GK,[8] corrected GK, and full expansion treatments of these polymorphic transitions appear in Tables IV and V and in Figs. 1–16. These three treatments all agree fairly well with experiment (except, as mentioned above, the full expansion treatment of RbI, where the theory predicts the $B2$ phase to be 0.3 kcal mole^{-1} more stable than the $B1$ phase, and KI), and as expected, are much more successful than most Born-Mayer semiempirical calculations.[6] The semiempirical

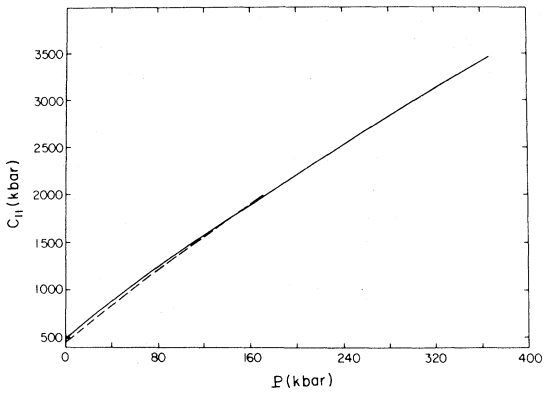

FIG. 17. Pressure variation of C_{11} in the $B1$ phase of NaCl: – – – First-nearest-neighbor-corrected GK model; —— Full expansion treatment using Eq. (21).

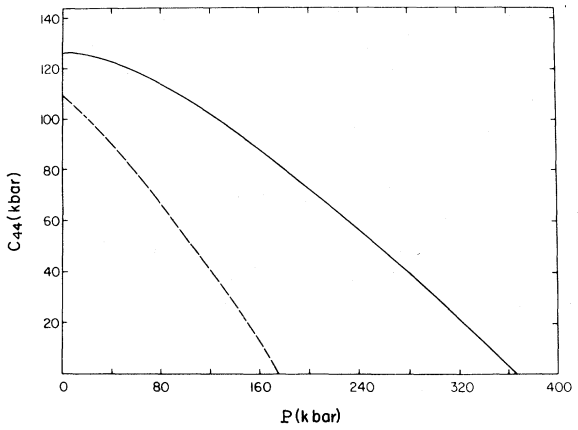

FIG. 19. Pressure variation of C_{44} in the $B1$ phase of NaCl.

expansions have usually been fitted to equilibrium properties of these crystals and hence cannot describe the behavior of the $B1$ phase under compression where interionic separations no longer correspond to their equilibrium values. An exception is the detailed semiempirical work of Tosi and Fumi,[7] where high-pressure parameters were used and which shows good agreement with experiment. The corrected GK and full expansion treatments predict relative volume factors for these transitions which show excellent agreement with experiment. For example, at the theoretical transition pressures of KBr, $-\Delta V_t/V_{01}$ is in the range from 10.5 to 12.7%, whereas experimentally, at the observed transition pressure it is 10.5%.[10] In addition, the phase diagrams for KCl and KBr agree favorably with the available compression results of Bridgman,[10] as do those of RbCl and RbBr, where fewer experimental data points are available.

For KCl, KBr, KI, RbCl, RbBr, and RbI, the rather small energy differences between the two phases generally leads to uncertainties in the theoretical transtion pressures, as has been described in detail by Gordon and Kim.[8] In addition, kinetic effects have been observed in these experiments[10] so that there are no unambiguous experimental transition pressures in these crystals. For example, Bassett *et al.*[1] have observed a $B1$-$B2$ poly-polymorphic transition in KCl near 21 kbar, rather than near 19 kbar as observed by Bridgman.[10] This therefore suggests that the observed transitions do not occur exactly at the thermodynamic phase boundary. For these two reasons, we do not expect complete agreement between our calculations and experiments.

In contrast to the polymorphic transitions described above, the $B1$-$B2$ phase change in NaCl occurs experimentally at 300 kbar, is rapid, reversible, exhibits little hysteresis effects, and has therefore been assumed by Bassett to lie close to the thermodynamic phase boundary.[3] In addition, the relative volume factor at the transition pressure is much less (at 3.7%) than those characteristic of the KCl, KBr, RbCl, and RbBr transitions. It is important to understand which forces are of importance in this transition because NaCl is often used as a marker or internal reference in diamond-anvil high-pressure cells. By following an equation of state (generally empirical or semiempirical), lattice parameters of the crystal observed by x-ray diffraction during a compression experiment may be converted to pressures reached during that compression. This transition has also been of interest because of conflicting experimental measurements. Initial studies of the crystal under dynamic shock-wave compression and by static methods revealed a $B1$-$B2$ phase change near 20 kbar.[4] This, of course, does not follow the energy-difference pattern established in Table III, nor does it agree with even the crudest semiempirical calculations. Detailed studies by Bassett partially resolved the problem and using a diamond-anvil high-pressure cell, a phase change at the more

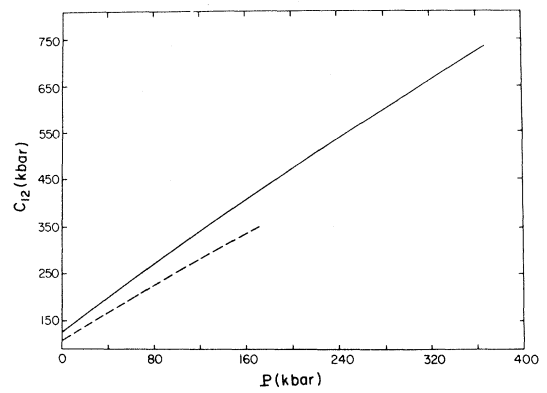

FIG. 18. Pressure variation of C_{12} in the $B1$ phase of NaCl.

reasonable value of 300 kbar was observed.[3] Further studies by Fritz *et al.* using shock waves showed close agreement with Bassett's results.[2]

Our calculations as summarized in Tables IV and V indicate that the full expansion treatment which predicts a transtion at 107 kbar, provides a better description of the crystal phases of NaCl than either semiempirical,[6] GK,[8] or corrected GK models can provide. Here the applied pressures are so high that the effect of second- and third-nearest-neighbor short-range interactions is of great importance, in contrast to the KCl, KBr, KI, RbCl, RbBr, and RbI transitions where these interactions were at large separations and hence of minor importance. From the phase diagram given in Fig. 6, it is seen that up to 100 kbar the full expansion treatment provides an excellent description of the $B1$ phase; hence it is believed that it is the theoretical description of the $B2$ phase that is incomplete. From Table IV it is seen that the theoretical relative volume factor at the transition pressure in this crystal is of the same order of magnitude as the experimental factor, and both differ greatly from the order of magnitude of the factors observed for those phase changes occurring in the 4 to 25 kbar range.

For those $B1$-$B2$ alkali-halide transitions which have yet to be experimentally observed, we expect the full expansion treatment to provide a more accurate description of the two phases than either a GK, corrected GK, or semiempirical treatment would. The results summarized in Tables IV and V seem to correlate with structural trends in these halides and with the energy-difference trends established in Table III. For NaF, in particular, for which no phase change has been observed experimentally to 200 kbar, it seems likely that the full expansion result of 326 kbar corresponds well with the actual transition pressure in this system, for NaCl transforms experimentally at 300 kbar and the fluoride should transform at a slightly greater pressure than the chloride. For LiCl, LiBr, and LiI, our predictions also seem plausible. For LiF the full expansion treatment predicts a phase change at 2900 kbar, which is much larger than semiempirical estimates; but semiempirical theories generally underestimate transition pressures in lithium salts,[6] and more detailed semiempirical treatments, which included nonadditive three-body forces, have predicted transitions at pressures in excess of 1000 kbar.[23] Nevertheless, as we have discussed before, three-body forces and covalent bonding may be of great importance in LiF; hence our prediction should be considered as only a rough estimate of the transition pressure in this crystal.

In all our phase diagrams, we have extended the curves for each phase beyond the theoretical transition pressures into regions of metastability. In these metastable regions, each crystal still lies at the bottom of its energy well. Nevertheless, the other crystal phase is the more stable. We believe that these metastable parts of the phase diagrams may be of great importance in shock-wave experiments. The $B1$-$B2$ phase transformations appear to proceed as a nucleation process. Around the transition pressure, nuclei of the second phase begin to form. This is then followed by surface growth of the $B2$ phase and later by the complete disappearance of the $B1$ phase. In those shock-wave or other experiments in which the crystal in its $B1$ phase is subjected to a large increase in pressure over a time scale so small as to preclude nucleation or surface extent, the crystal is following a path along the $B1$ curve in the phase diagram and sliding past the transition pressure into the metastable region. As the pressure decreases, the crystal then slides back along this curve to its zero-applied-pressure point. Hence these metastable extensions may be of importance to indicate whether in a high-pressure experiment the sample has not had enough time to respond and has moved past the transition pressure without exhibiting a phase change, or whether, indeed, insufficient pressure has been applied and the transition pressure has not yet been reached. These diagrams may also be of importance in geological processes.

C. Elastic constants of the $B1$ phase

We have shown that the cohesive energies, lattice constants, and high-pressure phase transformations of most of the alkali halides can be well described by assuming that the interionic interactions are pairwise additive and many-body effects may be neglected. The contribution of many-body forces in these crystals can be estimated by examining deviations from the Cauchy relation $C_{12} = C_{44}$. In cubic crystals, where the ions are centers of inversion symmetry, in the absence of zero-point motion and applied pressure, if the forces are of a central-pairwise-additive type the Cauchy relation is satisfied. Our model, of course, satisfies these criteria and as shown in Table VI, the relation holds for all the alkali halides in the $B1$ phase. Experimentally, for the static lattice the Cauchy relation is not rigorously satisfied due to contribution from many-body effects. In some crystals such as NaCl, comparison of experiment[20] and theory shows that the deviation from a two-body-force description is minor, whereas in crystals such as LiF, which we have discussed in detail above, many-body forces appear to be important. Many-body interactions in ionic crystals are more difficult to treat within the framework of an electron-gas approximation but fortunately, as shown in Table VI, in many cases a two-body description

appears adequate. A theoretical treatment of many-body effects in ionic crystals has been performed by Löwdin,[25] but his description of cohesive energies, lattice constants, high-pressure transitions, and bulk moduli shows poorer agreement with experiment than our present study shows.

There are two difficulties in comparing theoretical elastic constants with experiment. First, there are uncertainties in some of the measured elastic constants, particularly C_{12}. Whereas C_{11} and C_{44} may be determined directly by ultrasonic techniques which monitor particle motion longitudinal and transverse to the [100] propagation direction, C_{12} must be obtained from measurements of a linear combination of elastic constants with the crystal usually aligned in the [110] direction. Hence rather sizeable uncertainties estimated to be ±5% by Briscoe,[26] can be introduced into C_{12} obtained by taking the difference of large numbers. Briscoe has also noted that elastic constants exhibit a variation of 2%–3% from author to author. Our theoretical elastic constants have uncertainties of about 2% as well. For comparison with our calculations, we have listed what appear to be the most reliable values quoted by Simmons and Wang.[22,26–30,33,34]

The second difficulty, which is more serious, is that in many cases a direct comparison with experimental 4.2 °K elastic constants or constants extrapolated to 0 °K from a series of values at slightly higher temperatures is not rigorously correct.[31] Nor can conclusions about many-body forces be made by comparing raw low-temperature experimental C_{12} and C_{44} values, for while we have shown that zero-point motion is of minor importance to the cohesive energy, lattice constant, and transition pressure of an alkali halide, the Cauchy relations are for a *static* lattice; hence, correcting for zero-point motion is very important here. To test the Cauchy relations and to compare with our theoretical values, it is preferable to extrapolate high-temperature elastic constants ($T > \Theta_D$) to 0 °K.[31] Spetzler *et al.*[20] have performed this extrapolation for NaCl and have shown the Cauchy relation at 0 °K to be mildly violated ($C_{12} = 127$, $C_{44} = 140$ kbar), and we have performed similar extrapolations for a few of the other halides for which sufficient high-temperature experimental data could be obtained and have summarized the results in Table VI. By extrapolating data from the classical region, zero-point effects are largely removed from the 0 °K results, and yet very little anharmonic effects are introduced. For those cases for which an extrapolation could not be performed, a rough comparison with theory may be obtained from experimental 4.2 °K values.

The table shows that in most cases the calculated elastic constants and moduli show excellent agreement with experiment, generally to within 10%. This demonstrates the accuracy of the electron-gas description of the forces in these halides. In most cases the "complete" expansion treatment gives better agreement than the uncorrected GK model,[8] and most of the other theoretical models (which Briscoe[26] has evaluated) do. For all but the lithium halides (and NaF), the relation $C' > C_{44}$, which holds experimentally,[26] is seen to be obeyed. The reversal in lithium halides is due[15] to closer contact, due to short-range forces, between halide ions along the [110] direction than between alkali and halide ions along the [100] direction due to the small size of Li^+, C' being a shear constant associated with [110] direction, and C_{44} with that of the [100] direction.

Recently, experimental studies have been performed on the pressure variation of the elastic constants of NaCl. O'Connell *et al.* have performed static measurements to 10 kbar and plan to extend these to even higher pressures.[20,31] We have performed a pressure variation of the elastic constants of NaCl to the onset of a shear instability, $C_{44} = 0$, and have found the applied pressure form of the Cauchy relation,[35,36] $C_{12} - C_{44} = 2P$ valid for static-lattice central-force models under hydrostatic pressure P to hold. This theoretical study may be of importance to geophysicists interested in the behavior of crystals that exist under the high pressures of the earth's mantle and which are as yet experimentally inaccessible by present techniques. The results also provide an interesting further check on the adequacy of the electron-gas description of the NaCl $B1$ phase throughout a wide range of pressures.

In Sec. V B, we hypothesized that our description of the $B1$-$B2$ phase transformation in NaCl might be inaccurate due to an incomplete description of the $B2$ phase of the crystal. Comparison of our compression data with Bridgman's experimental $B1$ results[10] showed excellent agreement to 100 kbar, provided the full Eq. (2) was employed. Now supporting evidence may be obtained from Fig. 19. The onset of a shear instability, $C_{44} = 0$ here, should occur at a pressure higher than the transition pressure of the crystal which experimentally is at 300 kbar. Figure 19 shows that a first-nearest-neighbor-corrected GK model is inadequate, for it predicts a shear instability at 175 kbar; a Born-Mayer model with only first-nearest-neighbor short-range forces also predicts an instability in this range.[20] The full expansion treatment, however, predicts an instability at 370 kbar in a region similar to that predicted by a second-nearest-neighbor Born-Mayer model.[20] This supports our suggestion that although our model predicts a phase change at 107 kbar, rather less than experiment, the $B1$ phase of the crystal appears to be

adequately described by a two-body GK central-force model including second-nearest-neighbor interactions.

The rather good overall agreement between theory and experiment in alkali halides is encouraging, and it is hoped that we shall be able to extend the electron-gas model to a variety of other crystals.

ACKNOWLEDGMENTS

One of us (A. J. C.) would like to thank Marvin Waldman for discussing his electron-gas correction factor work prior to publication, and for many useful discussions of electron-gas theory, and William Swope for computational assistance. We would both like to thank Professor Richard J. O'Connell and Dr. Geoffrey Davies of the Geology Department at Harvard for many useful discussions and for providing experimental data for comparison with our calculations.

[1]W. A. Bassett, T. Takahashi, and J. K. Campbell, Trans. Am. Crystallogr. Assoc. 5, 93 (1969), and references therein.

[2]M. H. Rice, R. G. McQueen, and J. M. Walsh, Solid State Phys. 6, 1 (1958); J. N. Fritz, S. P. Marsh, W. J. Carter, and R. G. McQueen, Natl. Bur. Stand. Publ. No. 326 (U.S. GPO, Washington, D. C., 1971), p. 201.

[3]W. A. Bassett, T. Takahashi, H. K. Mao, and J. S. Weaver, J. Appl. Phys. 39, 319 (1968).

[4]V. V. Edmokimova and L. F. Vereshchagin, Zh. Eksp. Teor. Fiz. 43, 1208 (1962) [Sov. Phys.-JETP 16, 855 (1963)].

[5]R. B. Jacobs, Phys. Rev. 54, 468 (1938).

[6]M. Born and K. Huang, *Dynamic Theory of Crystal Lattices* (Oxford U. P., London, 1954).

[7]M. P. Tosi, Solid State Phys. 16, 1 (1964); M. P. Tosi and F. G. Fumi, J. Phys. Chem. Solids 23, 359 (1962).

[8]Y. S. Kim and R. G. Gordon, Phys. Rev. B 9, 3548 (1974), and references therein.

[9]R. G. Gordon and Y. S. Kim, J. Chem. Phys. 56, 3122 (1972).

[10]P. W. Bridgman, Proc. Am. Acad. Arts Sci. 76, 1 (1945).

[11]J. S. Cohen and R. T. Pack, J. Chem. Phys. 61, 2372 (1974), and references therein.

[12]M. Waldman and R. G. Gordon (unpublished).

[13]C. Kittel, *Introduction to Solid State Physics*, 4th Ed. (Wiley, New York, 1971), Chap. 3.

[14]C. W. F. Pistorius, J. Phys. Chem. Solids 25, 1477 (1964); 26, 1543 (1965); and J. Chem. Phys. 43, 1557 (1965).

[15]H. B. Huntington, Solid State Phys. 7, 213 (1958).

[16]M. Blackman, Proc. Phys. Soc. Lond. B 70, 827 (1957); Philos. Mag. 3, 831 (1958).

[17]K. Fuchs, Proc. Roy. Soc. A 153, 622 (1936); 157, 444 (1936).

[18]R. A. Cowley, Proc. Roy. Soc. A 268, 121 (1962).

[19]O. L. Anderson and R. C. Liebermann, Phys. Earth Planet. Inter. 3, 61 (1970).

[20]H. Spetzler, C. G. Sammis, and R. J. O'Connell, J. Phys. Chem. Solids 33, 1727 (1972).

[21]A. D. B. Woods, W. Cochran, and B. N. Brockhouse, Phys. Rev. 119, 980 (1960).

[22]G. Simmons and H. Wang, *Elastic Constants: Single Crystal Elastic Constants and Calculated Aggregate Properties* (M. I. T. U. P., Cambridge, 1971).

[23]L. Jansen and E. Lombardi, Discuss. Faraday Soc. 40, 78 (1965).

[24]A. J. Cohen (unpublished).

[25]P. O. Löwdin, Ph. D. thesis (Uppsala, 1948) (unpublished).

[26]J. T. Lewis, A. Lehoczky, and C. V. Briscoe, Phys. Rev. 161, 877 (1967).

[27]C. V. Briscoe and C. F. Squire, Phys. Rev. 106, 1175 (1957).

[28]M. H. Norwood and C. V. Briscoe, Phys. Rev. 112, 45 (1958).

[29]J. K. Galt, Phys. Rev. 73, 1460 (1948).

[30]C. Susse, J. Rech. Cent. Natl. Rech. Sci. 54, 23 (1961).

[31]R. J. O'Connell (private communication).

[32]S. N. Vaidya and G. C. Kennedy, J. Phys. Chem. Solids 32, 951 (1971).

[33]M. Ghafelehbashi, D. P. Dandekar, and A. L. Ruoff, J. Appl. Phys. 41, 652 (1970).

[34]R. Dalven and C. W. Garland, J. Chem. Phys. 30, 346 (1959).

[35]D. Lazarus, Phys. Rev. 76, 545 (1949).

[36]For $P > 0$ we have calculated, using the notation of Refs. 20 and 35, the effective elastic constants. These are described by D. C. Wallace, Phys. Rev. 162, 776 (1967), where they are denoted as B_{ij}.